Supplementary Material (ESI) for Chemical Communications

Oxovanadium(IV)-based near-IR PDT agents: design to biological evaluation

Pijus K. Sasmal,[a] Sounik Saha,[a] Ritankar Majumdar,[b] Rajan R. Dighe,[b] and Akhil R. Chakravarty*[a]

[a] *Department of Inorganic and Physical Chemistry, Indian Institute of Science and* [b] *Department of Molecular Reproduction, Development and Genetics, Indian Institute of Science, Bangalore 560012, India. E-mail: arc@ipc.iisc.ernet.in*

Electronic Supplementary Information (ESI)

Experimental Section

Materials and measurements. All reagents and chemicals were procured from commercial sources (SD Fine Chemicals, India; Aldrich, USA) and used without further purifications. Solvents used were purified by standard procedures.[S1] Syntheses of the complexes were done under nitrogen atmosphere using Schlenk technique. Supercoiled (SC) pUC19 DNA (cesium chloride purified) was purchased from Bangalore Genie (India). Tris-(hydroxylmethyl)aminomethane-HCl (Tris-HCl) buffer solution was prepared using deionized and sonicated triple distilled water. Calf thymus (CT) DNA, agarose (molecular biology grade), distamycin-A, catalase, superoxide dismutase (SOD), 2,2,6,6-tetramethyl-4-piperidone (TEMP), 1,4-diazabicyclo-[2.2.2]octan (DABCO), ethidium bromide (EB), bovine serum albumin (BSA), lysozyme, acrylamide, N,N'-methylenebisacrylamide, ammonium persulphate, N,N,N′,N′-tetramethylethylenediamine (TEMED), 2-mercaptoethanol (MPE), Tricine, glycerol, sodium dodecyl sulphate (SDS), bromophenol blue, coomassie brilliant blue R-250 were from Sigma (USA). The *N,N*-donor heterocyclic bases dipyrido-[3,2-d:2′,3′-f]-quinoxaline (dpq) and dipyrido[3,2-a:2′,3′-c]phenazine (dppz) were prepared by literature procedures using 1,10-phenanthroline-5,6-dione as a precursor reacted with ethylenediamine for dpq and 1,2-phenylenediamine for dppz.[S2,S3]

The elemental analysis was done using a Thermo Finnigan Flash EA 1112 CHNS analyzer. The infrared and electronic spectra were recorded on Perkin Elmer Lambda 35 and Perkin Elmer Spectrum one 55 spectrophotometers, respectively. Molar conductivity measurements were performed using a Control Dynamics (India) conductivity meter. Room temperature magnetic susceptibility data were obtained from a George Associates Inc. Lewis-coil force magnetometer using $Hg[Co(NCS)_4]$ as a standard. Experimental susceptibility data were corrected for diamagnetic contributions.[S4] Cyclic voltammetric measurements were made at 25 °C on a EG&G PAR Model 253 Versa Stat potentiostat/galvanostat with electrochemical analysis software 270 using a three electrode set-up comprising of a glassy carbon working, platinum wire auxiliary and a saturated calomel reference (SCE)

electrode. Potassium chloride (KCl, 0.1 M) was used as a supporting electrolyte in DMF-water (v/v 1:5). The electrochemical data were uncorrected for junction potentials. Electrospray ionization mass spectral measurements were done using Esquire 3000 plus ESI (Bruker Daltonics) and Q-TOF Mass Spectrometer. Fluorescence microscopic investigations were carried out on Leica DM IL microscope with integrated Leica DFC400 camera and IL50 image software.

Preparation of $[VOClB_2]Cl$ (B = dpq, 1; **dppz, 2).** The complexes were prepared by a general synthetic procedure in which a mixture of the vanadium(III) chloride (0.07 g, 0.5 mmol) and heterocyclic base [0.23 g, dpq (**1**); 0.29 g, dppz (**2**), (1.0 mmol)] was taken in 20 mL of methanol. The resulting solution was stirred at room temperature for three hour. A clear purple solution was obtained after stirring the mixture for 3h. The reaction mixture was kept for recrystallizaion at room temperature and a green solid was appeared [Yield: ~ 80%]. The complex in its PF_6 salt was prepared for crystallographic study. Anal. Calcd for $C_{28}H_{16}N_8OCl_2V$ (**1**): C, 55.83; H, 2.68; N, 18.60. Found: C, 55.71; H, 2.62; N, 18.63. ESI-MS in MeOH: m/z 566 $[M]^+$. Λ_M = 84 S m^2 M^{-1} in DMF at 25 ºC. IR (KBr phase, cm^{-1}): 3401br, 3073w, 1620w, 1484m, 1403s, 1085m, 978s (V=O), 818m, 733m (br, broad; s, strong; m, medium; w, weak). UV-vis in 15% DMF-Tris-HCl buffer (pH 7.2) [λ_{max}/nm (ε/$dm^3mol^{-1}cm^{-1}$)]: 712 (30), 525 (56), 434 (260), 341 (6740), 327 (8880) and 254 (52480). μ_{eff} = 1.63 μ_B at 298 K. Anal. Calcd for $C_{36}H_{20}N_8OCl_2V$ (**2**): C, 61.55; H, 2.87; N, 15.95. Found: C, 61.51; H, 2.78; N, 15.88. ESI-MS in MeOH: m/z 666 $[M]^+$. Λ_M = 74 S m^2 M^{-1} in DMF at 25 ºC. IR (KBr phase, cm^{-1}): 3408br, 3080w, 1621m, 1497s, 1419m, 1358w, 1079w, 979s (V=O), 772m, 732s. UV-vis in 15% DMF-Tris-HCl buffer (pH 7.2) [λ_{max}/nm (ε/$dm^3mol^{-1}cm^{-1}$]: 715 (32), 528 (70), 452 (280), 380 (11460), 363 (12300) and 267 (54090). μ_{eff} = 1.66 μ_B at 298 K.

Solubility and stability. The complexes were soluble in H_2O, MeOH, DMF, DMSO; less soluble in MeCN, CH_2Cl_2 and insoluble in hydrocarbon solvents. They were stable in both the solid and solution phases.

X-ray crystallographic procedures. The crystal structure of $[VOCl(dpq)_2](PF_6)$ (**1a**) was obtained by single crystal X-ray diffraction technique. Crystals were obtained from MeOH solution of the complex in the presence of NH_4PF_6 on slow evaporation of the solvent. Crystal mounting was done on glass fibre with epoxy cement. All geometric and intensity data were collected at room temperature using an automated Bruker SMART APEX CCD diffractometer equipped with a fine focus 1.75 kW sealed tube Mo-K_α X-ray source (λ = 0.71073 Å) with increasing ω (width of 0.3° per frame) at a scan speed of 5 seconds per frame. Intensity data, collected using ω-2θ scan mode, were corrected for Lorentz–polarization effects and for absorption.[S5] Structure was solved by the combination of Patterson and Fourier techniques and refined by full-matrix least-squares method using SHELX system of programs.[S6] All hydrogen atoms belonging to the complex were in their calculated positions and refined using a riding model. All non-hydrogen atoms were refined anisotropically. Perspective view of the molecule was obtained by ORTEP.[S7] The solvent non-hydrogen atoms of MeCN were refined isotropically. The hydrogen atoms of MeCN were not located due to high thermal motion of the carbon atom of the methyl group.

The structure of **2** was generated from the atomic coordinates of **1a** using Gaussview and then it was optimized using the hybrid HF-DFT method (B3LYP) using 6-31G basis set.[S8,S9] The calculation was done using Gaussian 03 program package.[S10]

DNA binding methods. The experiments were carried out in Tris-HCl buffer (5 mM Tris-HCl, pH 7.2) using the complex solution in DMF (1.5%) The calf thymus (CT) DNA (ca. 350 μM NP) in the buffer medium gave a ratio of UV absorbance at 260 and 280 nm of ca. 1.9:1 suggesting the DNA apparently free from protein. The concentration of DNA was estimated from its absorption intensity at 260 nm with a known molar absorption coefficient value of 6600 $dm^3\ mol^{-1}\ cm^{-1}$.[S11] Absorption titration experiments were performed by varying the concentration of the CT DNA while keeping the complex concentration as constant. Due correction was made for the absorbance of DNA itself. The spectra were recorded after equilibration for 5 min. The intrinsic equilibrium binding constant (K_b) and the binding

site size (s) of the complexes to CT DNA were obtained by McGhee-von Hippel (MvH) method using the expression of Bard and co-workers by monitoring the change of the absorption intensity of the spectral bands with increasing concentration of CT DNA by regression analysis using equation (1)

$(\varepsilon_a-\varepsilon_f)/(\varepsilon_b-\varepsilon_f) = (b-(b^2 - 2K_b^2C_t[DNA]_t/s)^{1/2})/2K_bC_t$, -------(1)

$b = 1 + K_bC_t + K_b[DNA]_t/2s$,

where ε_a is the extinction coefficient observed for the charge transfer absorption band at a given DNA concentration, ε_f is the extinction coefficient of the complex free in solution, ε_b is the extinction coefficient of the complex when fully bound to DNA, K_b is the equilibrium binding constant, C_t is the total metal complex concentration, $[DNA]_t$ is the DNA concentration in nucleotides and *s* is the binding site size in base pairs.[S12,S13] The non-linear least-squares analysis was done using Origin Lab, version 6.1.

DNA melting experiments were carried out by monitoring the absorption intensity of CT DNA (170 μM) at 260 nm at various temperatures, both in the absence and presence of the oxovanadium(IV) complexes (10 μM). Measurements were carried out using a Cary 300 bio UV-vis spectrometer with a Cary temperature controller with increasing the temperature of the solution by 0.5 °C per min. Viscometric titrations were performed with a Schott Gerate AVS 310 Automated Viscometer. The viscometer was thermostated at 37 ºC in a constant temperature bath. The concentration of CT DNA was 140 μM in NP and the flow times were measured with an automated timer, and each sample was measured 3 times, and an average flow time was calculated. Data were presented as $(\eta/\eta_0)^{1/3}$ vs. [complex]/[DNA], where η is the viscosity of DNA in the presence of complex and η_0 is that of DNA alone. Viscosity values were calculated from the observed flowing time of DNA-containing solutions (t) corrected for that of the buffer alone (t_0), $\eta = (t - t_0)/t_0$.

DNA cleavage experiments. The cleavage of supercoiled pUC19 DNA (30 μM, 0.2 μg, 2686 base-pair) was studied by agarose gel electrophoresis using metal complexes in 50 mM tris(hydroxylmethyl)methane-HCl (Tris-HCl) buffer (pH 7.2) containing 50 mM NaCl. For photo-

induced DNA cleavage studies, the reactions were carried out under illuminated conditions using UV-A source at 365 nm (6 W, Model LF-206.LS) or near IR light of >750 nm using a Spectra Physics Water-Cooled Mixed-Gas Ion Laser Stabilite® 2018-RM (Continuous-wave (CW) beam diameter at $1/e^2$ 1.8 mm ± 10% and beam divergence with full angle 0.7 mrad ± 10%) with an attachment Model 2018-RM-IR with all-lines IR optics (752.5–799.3 nm). The laser beam power at the sample position (5 cm from the aperture with a solution path length of 5 mm) was 100 mW, measured using Spectra Physics CW Laser Power Meter (Model 407A). After light exposure, each sample was incubated for 1.0 h at 37 °C and analyzed for the photo-cleaved products using gel electrophoresis. The mechanistic studies were carried out using different additives (NaN_3, 0.2 mM; DMSO, 4 μL; KI, 0.2 mM; catalase, 4 units; SOD, 4 units; TEMP, 0.2 mM; DABCO, 0.2 mM) prior to the addition of the complex. For the D_2O experiment, this solvent was used for dilution of the sample to 20 μL. The samples after incubation in a dark chamber were added to the loading buffer containing 0.25% bromophenol blue, 0.25% xylene cyanol, 30% glycerol (3 μL) and the solution was finally loaded on 1% agarose gel containing 1.0 μg/mL ethidium bromide. Electrophoresis was carried out in a dark chamber for 2.0 h at 60 V in TAE (Tris-acetate EDTA) buffer. Bands were visualized by UV light and photographed. The extent of DNA cleavage was measured from the intensities of the bands using UVITEC Gel Documentation System. Due corrections were made for the low level of nicked circular (NC) form present in the original supercoiled (SC) DNA sample and for the low affinity of EB binding to SC compared to NC and linear forms of DNA.[S14] The concentrations of the complexes and additives corresponded to that in the 20 μL final volume of the sample using Tris buffer. The observed error in measuring the band intensities was ~5%.

BSA binding experiments. The protein binding study was performed by tryptophan fluorescence quenching experiments using bovine serum albumin (BSA, 2 μM) as the substrate in phosphate buffer (pH 6.8). Quenching of the emission intensity of tryptophan residues of BSA at 344 nm (excitation wavelength at 295 nm) was monitored using complexes **1** and **2** as quenchers with increasing complex

concentration.[S15] Stern-Volmer I_0/I vs. [complex] plots were constructed using the corrected fluorescence data taking into account the effect of dilution. Linear fit of the data using Stern-Volmer equation ($I_0/I = 1 + K_{BSA}[Q]$), where I_0 and I are the emission intensity of BSA in the absence of quencher and emission intensity of BSA in the presence of the quencher of concentration [Q] gave the binding constant (K_{BSA}) values (using Origin 6.1).

Protein cleavage experiments. Photo-induced protein cleavage experiments were carried out according to the literature procedure described by Kumar and coworkers.[S16] Freshly prepared solution of BSA in 50 mM Tris-HCl buffer (pH 7.2) was used for the photochemical protein cleavage studies. The protein solutions in Tris-HCl buffer medium containing complexes **1** and **2** with varied concentration from 25 – 100 μM for BSA (5 μM) and lysozyme (10 μM) were photo-irradiated at 365 nm (6 W) for 2 h. Eppendorf vials were used for the UV-A light-induced protein cleavage studies. The BSA and lysozyme solution in the presence of the complexes were incubated at 37 °C for 1 h prior to the photo-exposure. The irradiated samples (50 μL) were dried in a centrifugal vaporizer EYELA Centrifugal Vaporizer (Model CVE-200D) and the samples were dissolved in the loading buffer (24 μL) containing SDS (7% w/v), glycerol (4% w/v), Tris-HCl buffer (50 mM, pH 6.8), mercaptoethanol (2% v/v) and bromophenol blue (0.01% w/v). The protein solutions were then denatured on heating to boil for 3 min. Samples were loaded on a 3% polyacrylamide (stacking) gel. The gel electrophoresis was done at 60 V until the dye passed into the separating gel from the stacking (3%) gel, and then the voltage was increased to 120 V. The gels were run for 1.5 h, stained with Coomassie Brilliant Blue R-250 solution (acetic acid/methanol/water = 1:2:7 v/v) and destained with water/methanol/acetic acid mixture (5:4:1 v/v) for 4 h. The gels, after destaining, were scanned with a HP Scanjet G3010 scanner and the images were further processed using Adobe Photoshop 7.0 software package. Molecular weight markers were used in each gel to calibrate the molecular weights of the BSA. The presence of reactive oxygen species was investigated by carrying out the photo-induced protein cleavage experiments. Various singlet oxygen quenchers like NaN_3 (3 mM), TEMP (3 mM) and hydroxyl radical scavengers like DMSO (20

μL) and KI (3 mM) were used for mechanistic studies. For lysozyme, 16.5% / 4% Tricine SDS-PAGE was performed after photoexposure following reported procedures.[S17]

Cell cytotoxicity assay. The phototoxicity of the complexes were assessed using the MTT assay based on the ability of mitochondrial dehydrogenases in the viable cells to cleave the tetrazolium rings of MTT forming dark blue membrane impermeable crystals of formazan which can be quantified at 595 nm on detergent solubulization.[S18] The level of the formazan product formed is a measure of the number of viable cells. Approximately, 8000 cells of human cervical carcinoma (HeLa) were plated in 96 wells culture plate in DMEM containing 10% FBS and after 24 h of incubation at 37 °C in CO_2 incubator, different concentrations of the vanadium complexes dissolved in 1% DMSO were added to the cells and incubation was continued for 30 min in dark. After incubation, the medium was replaced with PBS and photo-irradiated with a UV-A (365 nm) light (Fluence rate: 610 μW cm^{-2} for 15 min, 0.549 J cm^{-2}) or filtered (400-700 nm) visible light from a 300 W tungsten lamp (Fluence rate: 6.8 mW cm^{-2}) to provide a total dose of 20 J cm^{-2}. Post irradiation, PBS was replaced with DMEM-FBS and incubation was continued for further 12 h in dark. At the end of this incubation, 20 μL of 5 mg mL^{-1} of Thiazolyl blue tetrazolium bromide (MTT) was added to each well and incubated for an additional 3 h. The culture medium was discarded and 200 μL of DMSO was added to dissolve the formazan crystals and the abosorbance at 595 nm was determined using a BIORAD ELISA plate reader. Cytotoxicity of the test compounds was measured as the percentage ratio of the absorbance of the treated cells to the untreated controls. The IC_{50} values were determined by nonlinear regression analysis (GraphPad Prism). The UV-A light source used was a 6 W power tube of 365 nm from UVITEC, U.K. The power at the samples at a distance of 15 cm from the source was 610 μW cm^{-2}. The incoherent visible light source used for cytotoxicity and other cellular experiments consisted a 300 W tungsten lamp. The light was passed through a 400-700 nm broadband filter (Hot mirror, Newport U.S.A) followed by a 2 cm thick layer of water to avoid heating of the samples. The total distance of the samples from the light source

was 20 cm and the power at the sample was 6.8 mW cm^{-2}. The power at the samples was measured with a visible light meter from Spectra Physics.

References:

(S1) D. D. Perrin, W. L. F. Armarego and D. R. Perrin, *Purification of Laboratory Chemicals*; Pergamon Press: Oxford, 1980.

(S2) J. E. Dickeson, L. A. Summers, *Aus. J. Chem*., 1970, **23**, 1023-1027.

(S3) E. Amouyal, A. Homsi, J.–C. Chambron and J.–P. Sauvage, *J. Chem. Soc., Dalton Trans.* 1990, 1841-1845.

(S4) O. Khan, *Molecular Magnetism*, VCH, Weinheim, 1993.

(S5) N. Walker and D. Stuart, *Acta Crystallogr.,* 1983, **A39**, 158-166.

(S6) G. M. Sheldrick, *SHELX-97, Programs for Crystal Structure Solution and Refinement*; University of Göttingen, Göttingen, Germany, 1997.

(S7) C. K. Johnson, *ORTEP, Report ORNL-5138*; Oak Ridge National Laboratory: Oak Ridge, TN, 1976.

(S8) W. Hehre, L. Radom, P. v. R. Schleyer and J. A. Pople, *Ab Initio Molecular Orbital Theory*; Wiley: New York, 1986.

(S9) A. D. Becke, *J. Chem. Phys.,* 1993, **98**, 5648-5652.

(S10) M. J. Frisch, G. W. Trucks, H. B. Schlegel, G. E. Scuseria, M. A. Robb, J. R. Cheeseman, J. A. Jr. Montgomery, T. Vreven, K. N. Kudin, J. C. Burant, J. M. Millam, S. S. Iyengar, J. Tomasi, V. Barone, B. Mennucci, M. Cossi, G. Scalmani, N. Rega, G. A. Petersson, H. Nakatsuji, M. Hada, M. Ehara, K. Toyota, R. Fukuda, J. Hasegawa, M. Ishida, T. Nakajima, Y. Honda, O. Kitao, H. Nakai, M. Klene, X. Li, J. E. Knox, H. P. Hratchian, J. B. Cross, V. Bakken, C. Adamo, J. Jaramillo, R. Gomperts, R. E. Stratmann, O. Yazyev, A. J. Austin, R. Cammi, C. Pomelli, J. W. Ochterski, P. Y.

Ayala, K. Morokuma, G. A. Voth, P. Salvador, J. J. Dannenberg, V. G. Zakrzewski, S. Dapprich, A. D. Daniels, M. C. Strain, O. Farkas, D. K. Malick, A. D. Rabuck, R K. aghavachari, J. B. Foresman, J. V. Ortiz, Q. Cui, A. G. Baboul, S. Clifford, J. Cioslowski, B. B. Stefanov, G. Liu, A. Liashenko, P. Piskorz, I. Komaromi, R. L. Martin, D. J. Fox, T. Keith, M. A. Al-Laham, C. Y. Peng, A. Nanayakkara, M. Challacombe, P. M. W.Gill, B. Johnson, W. Chen, M. W. Wong, C. Gonzalez and J. A. Pople, *Gaussian 03*, revision C.02; Gaussian, Inc.: Wallingford, CT, 2004.

(S11) M. E. Reichman, S. A. Rice, C. A. Thomas and P. Doty, *J. Am. Chem. Soc.,* 1954, **76**, 3047-3053.

(S12) J. D. McGhee and P. H. von Hippel, *J. Mol. Biol.,* 1974, **86**, 469-489.

(S13) M. T. Carter, M. Rodriguez and A. J. Bard, *J. Am. Chem. Soc.,* 1989, **111**, 8901-8911.

(S14) J. Bernadou, G. Pratviel, F. Bennis, M. Girardet and B. Meunier, *Biochemistry* 1989, **28**, 7268-7275.

(S15) Y. J. Hua, Y. Liua, J. B. Wangb, X. H. Xiaob and S. S. Qua, *J. Pharm. Biomed. Anal.,* 2004, **36**, 915–919.

(S16) C. V. Kumar, A. Buranaprapuk, H. C. Sze, S. Jockusch and N. J. Turro, *Proc. Natl. Acad. Sci. U.S.A.,* 2002, **99**, 5810-5815.

(S17) H. Schägger and G. von Jagow, *Anal. Biochem.,* 1987, **166**, 368–379.

(S18) T. Mosmann, *J. Immunol. Methods,* 1983, **65**, 55-63.

Table S1. Selected crystallographic data for $[VOCl(dpq)_2]PF_6$ (**1a**·MeCN)

	1a·MeCN
Empirical formula	$C_{30}H_{19}ClF_6N_9OPV$
Formula weight	752.90
Temperature	293(2) K
Wavelength	0.71073 Å
Crystal system, space group	Triclinic, *P*-1
Unit cell dimensions	a = 11.087(7) Å, b = 12.192(7) Å , c = 12.471(8) Å
	α = 68.222(9)º, β = 81.920(10)º, γ = 87.459(10)º
Volume	1549.9(16) $Å^3$
Z	2
Calculated density	1.613 g cm^{-3}
Absorption coefficient	0.537 mm^{-1}
$F_{(000)}$	758
Crystal size	0.41 x 0.32x 0.25 mm^3
Theta range for data collection	1.77 to 25.0 º
Limiting indices	-13<=h<=13, -14<=k<=14, -14<=l<=14
Reflections collected / unique	14512 / 5446 [R(int) = 0.0668]
Completeness to theta = 25.00	99.7 %
Refinement method	Full-matrix least-squares on F^2
Data / restraints / parameters	5446 / 0 / 427
Goodness-of-fit on F^2	1.037
Final R indices [$I>2\sigma(I)$]	$R1$ = 0.0934, $wR2$ = 0.2540
R indices (all data)	$R1$ = 0.1475, $wR2$ = 0.2896
Largest diff. peak and hole	0.876 and -0.459 e. $Å^{-3}$

[a] $R = \Sigma||F_o|-|F_c||/\Sigma|F_o|$, [b] $wR = \{\Sigma[w(F_o^2-F_c^2)^2]/\Sigma[w(F_o)^2]\}^{½}$; $w = [\sigma^2(F_o)^2 + (AP)^2 + BP]^{-1}$, where $P = (F_o^2 + 2F_c^2)/3$; A and B values are 0.1560 and 1.8590, respectively.

Table S2. Selected bond distances (Å) and angles (deg.) for $[VOCl(dpq)_2]PF_6$ (**1a**·MeCN) with e.s.d.s in the parenthesis

	1a·MeCN
V(1)-O(1)	1.685(4)
V(1)-N(1)	2.120(6)
V(1)-N(5)	2.132(6)
V(1)-N(6)	2.160(6)
V(1)-N(2)	2.282(6)
V(1)-Cl(1)	2.286(3)
O(1)-V(1)-N(1)	93.9(2)
O(1)-V(1)-N(5)	99.6(2)
N(1)-V(1)-N(5)	164.1(2)
O(1)-V(1)-N(6)	96.4(2)
N(1)-V(1)-N(6)	93.7(2)
N(5)-V(1)-N(6)	76.5(2)
O(1)-V(1)-N(2)	166.3(2)
N(1)-V(1)-N(2)	73.81(19)
N(5)-V(1)-N(2)	91.8(2)
N(6)-V(1)-N(2)	78.7(2)
O(1)-V(1)-Cl(1)	100.95(17)
N(1)-V(1)-Cl(1)	92.57(15)
N(5)-V(1)-Cl(1)	93.08(17)
N(6)-V(1)-Cl(1)	161.10(17)
N(2)-V(1)-Cl(1)	85.97(16)

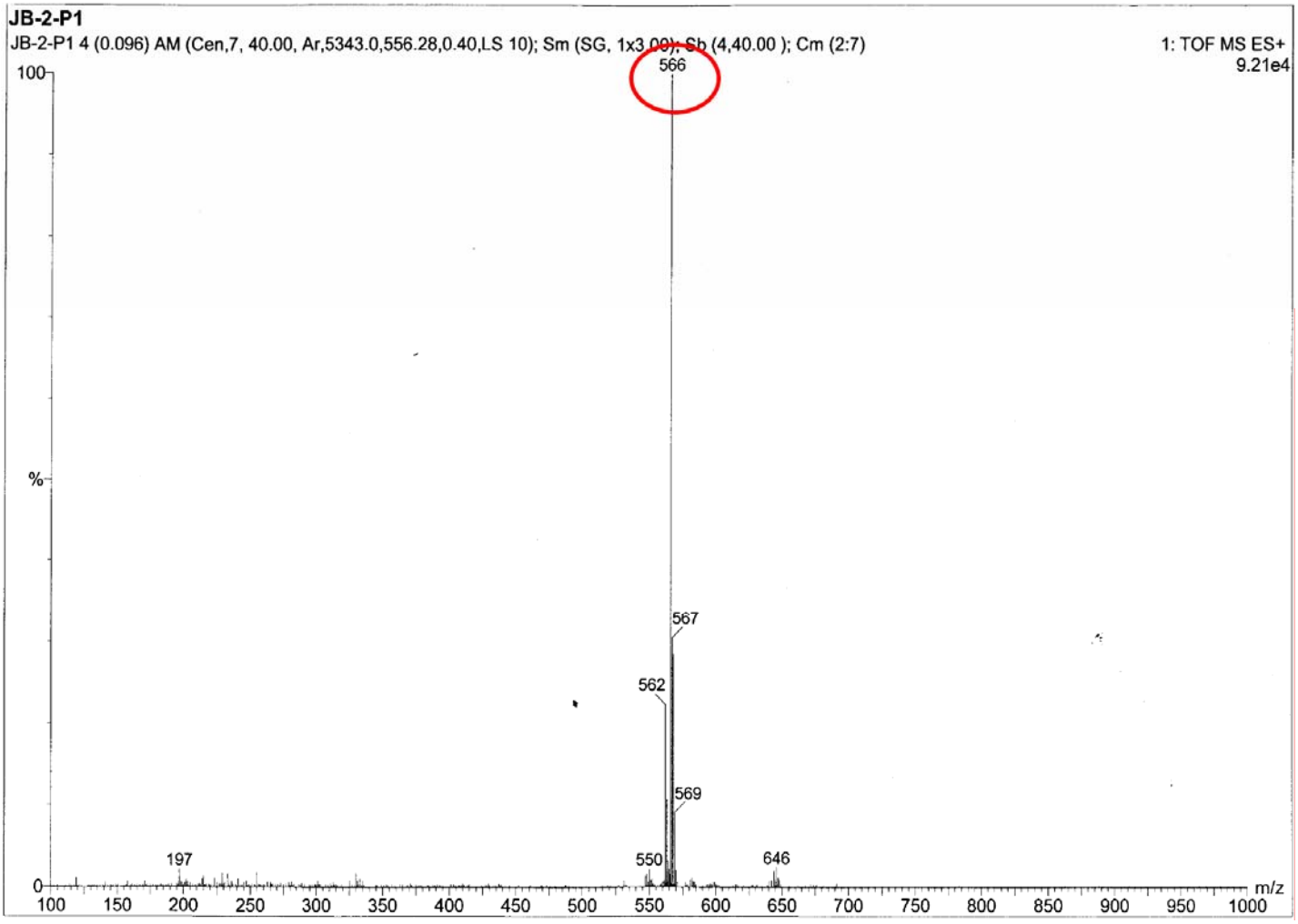

Fig. S1. The ESI-MS spectrum of the complex **1** showing the parent ion peak at 566 (m/z) in MeOH**.**

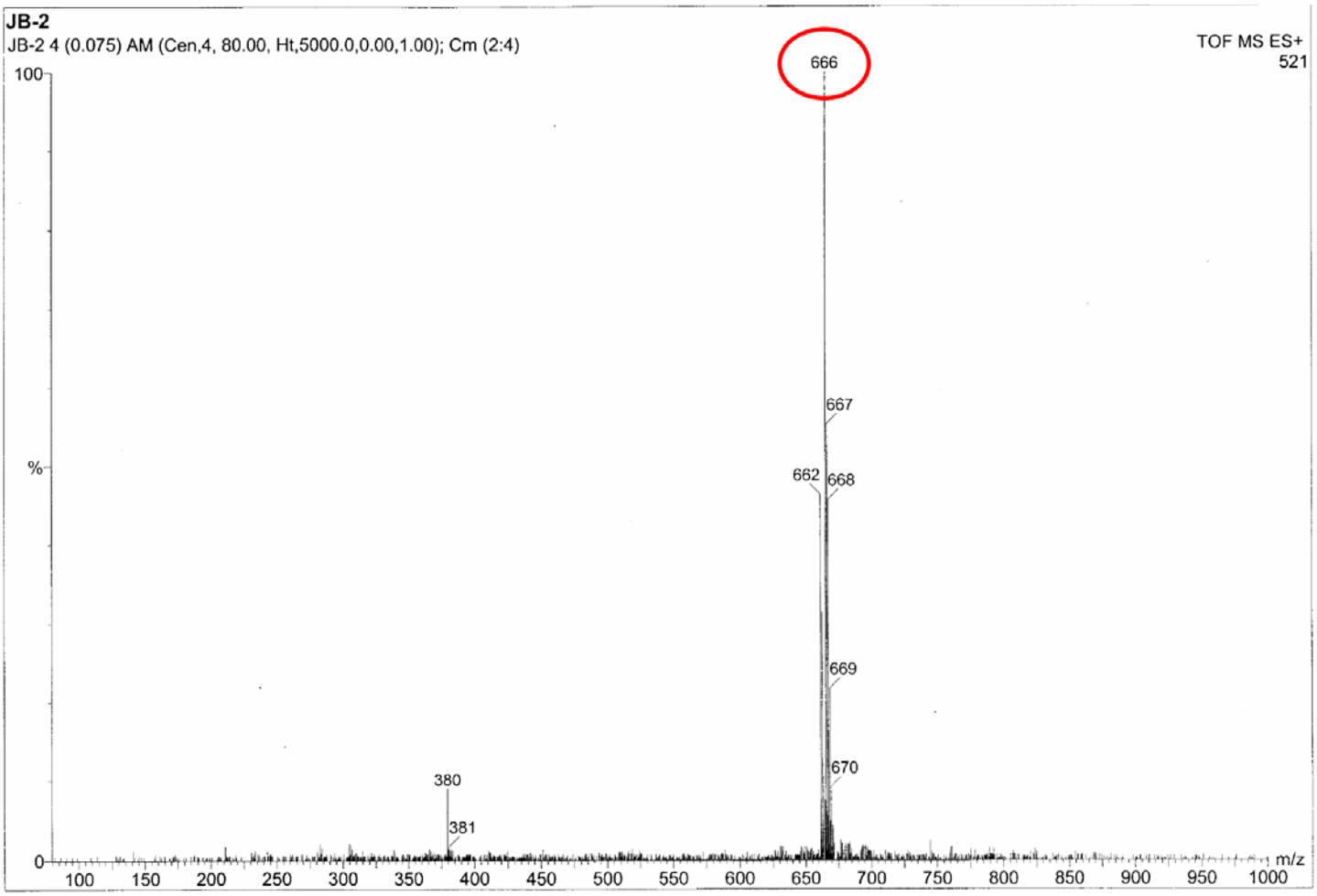

Fig. S2. The ESI-MS spectrum of the complex **2** showing the parent ion peak at 666 (m/z) in MeOH.

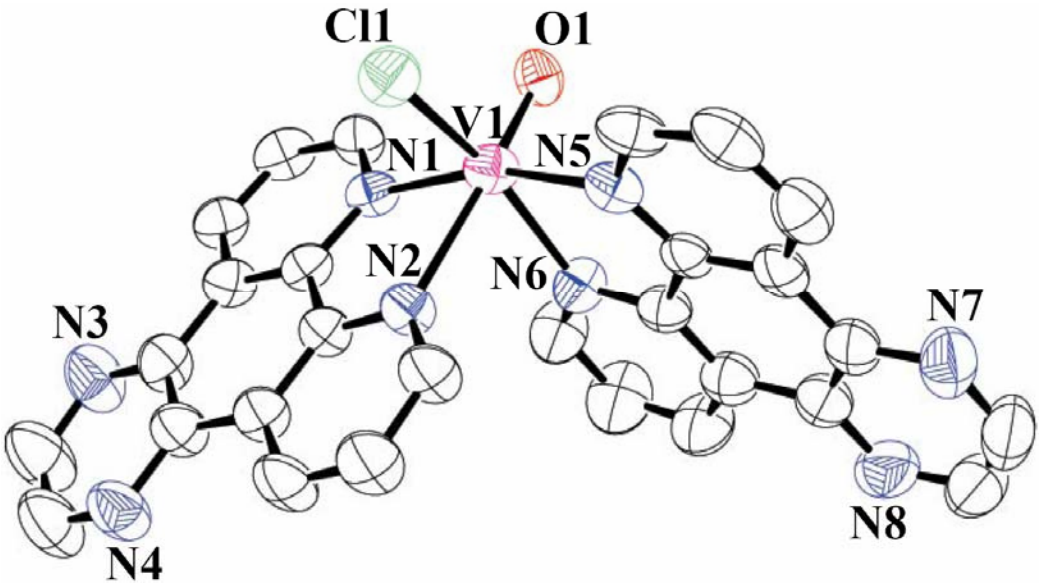

Fig. S3. ORTEP view of the cationic complex in $[VOCl(dpq)_2](PF_6)$ (**1a**·MeCN) showing atom labeling for only the metal and heteroatoms and 50% probability thermal ellipsoids. The hydrogen atoms are omitted from the diagram for clarity.

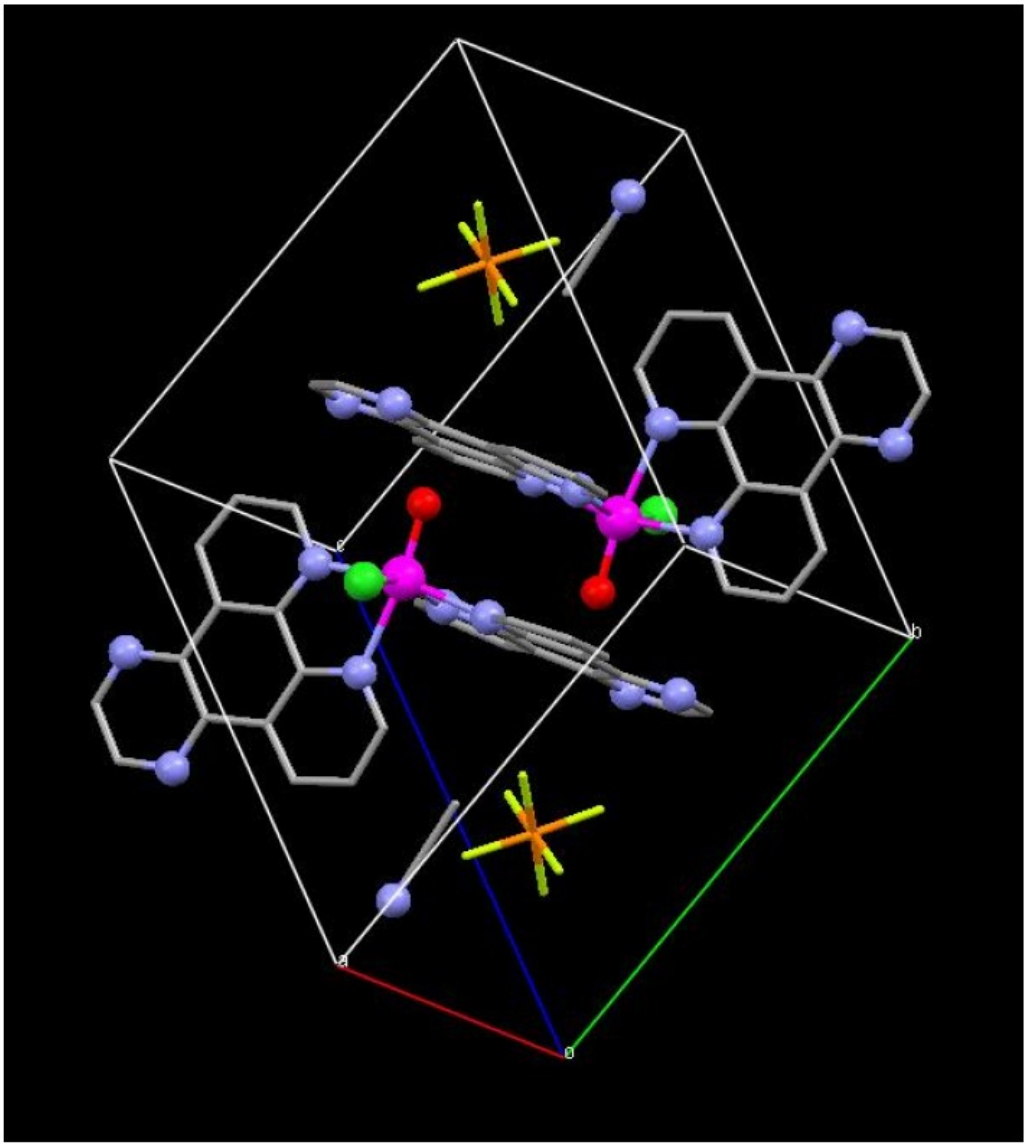

Fig. S4. Unit cell packing diagram of $[VOCl(dpq)_2](PF_6)$ (**1a**·MeCN).

Fig. S5. The energy-minimized structure of **2** was generated using the atomic coordinates of $[VOCl(dpq)_2](PF_6)$ (**1a**·MeCN). The *cis*-isomer is more stable (-3300.365068 Hartree mol^{-1}) than its corresponding *trans*-isomer (-3300.344440 Hartree mol^{-1}). The *cis*-isomer is 12.94 kcal mol^{-1} lower in energy than its corresponding *trans*-isomer. Energy minimization was done using the procedures as given in S8-S10.

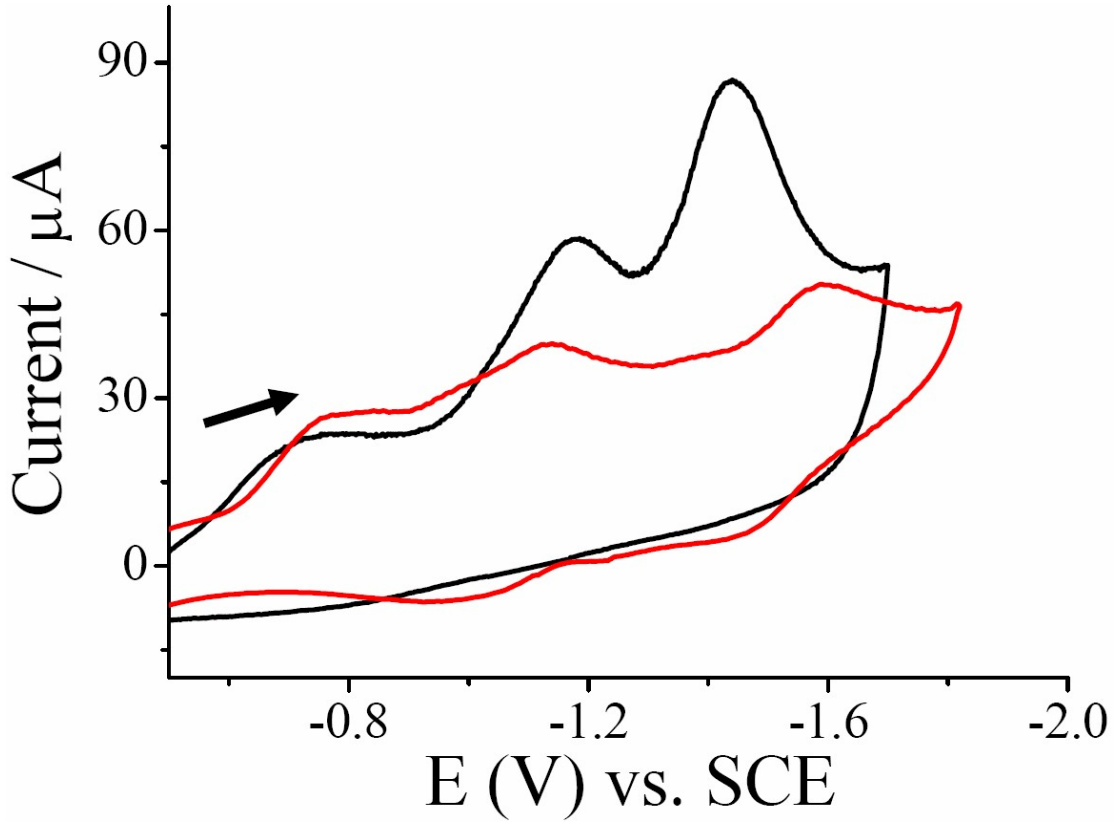

Fig. S6. Cyclic voltammograms of the complexes (**1**) (—) and (**2**) (—) in 20% DMF-Tris-HCl buffer at a scan speed of 50 mV s^{-1} and 0.1mol KCl as a supporting electrolyte. The voltammograms at ~ -0.7 V are assignable to the V(IV)-V(III) redox couple, whereas the voltammograms in the range of -1.0 to -1.8 V are due to ligand reductions.

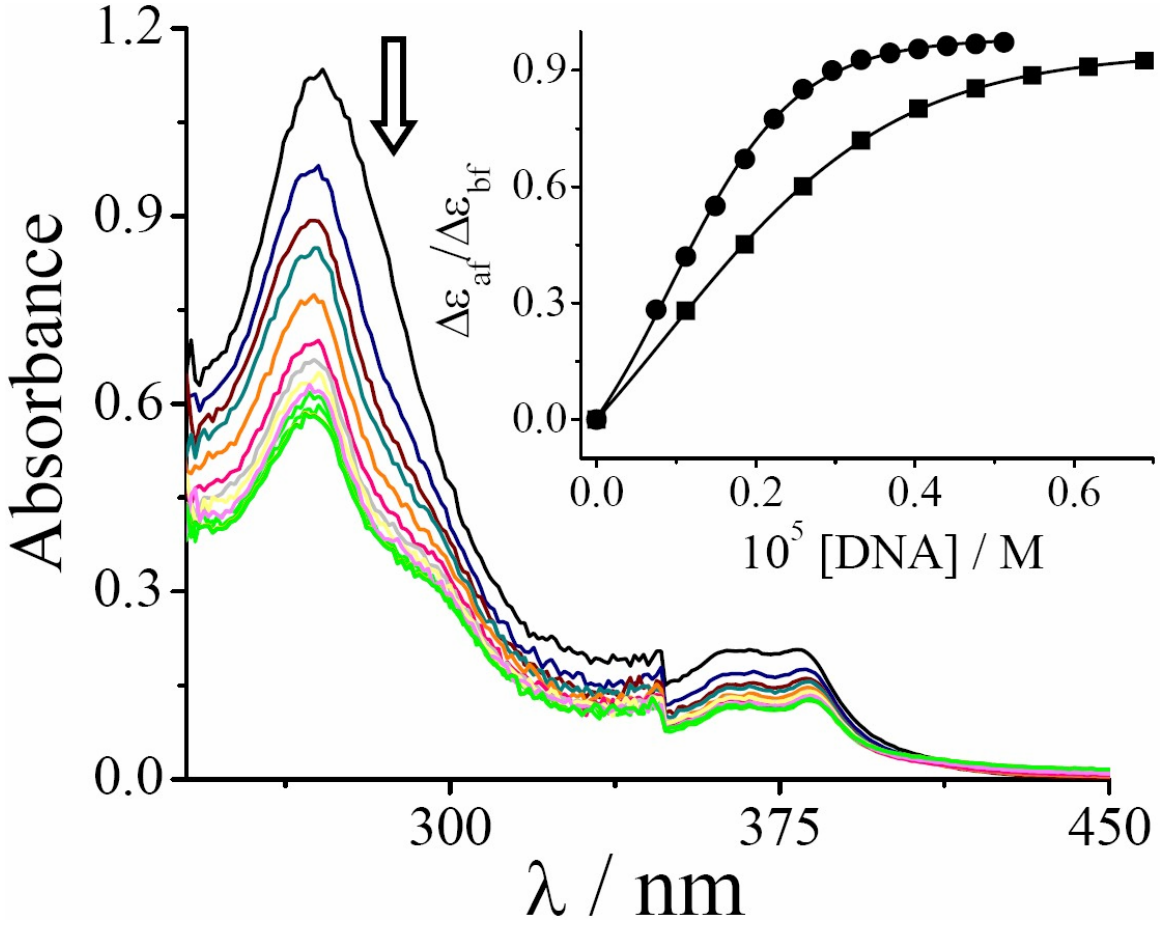

Fig. S7. Absorption spectral traces of the complex **2** in 5 mM Tris-HCl buffer (pH 7.2) on increasing the quantity of CT DNA. The inset shows the least-squares fits of $\Delta\varepsilon_{af}/\Delta\varepsilon_{bf}$ vs. [DNA] for **1** (■), **2** (●) using MvH equation.

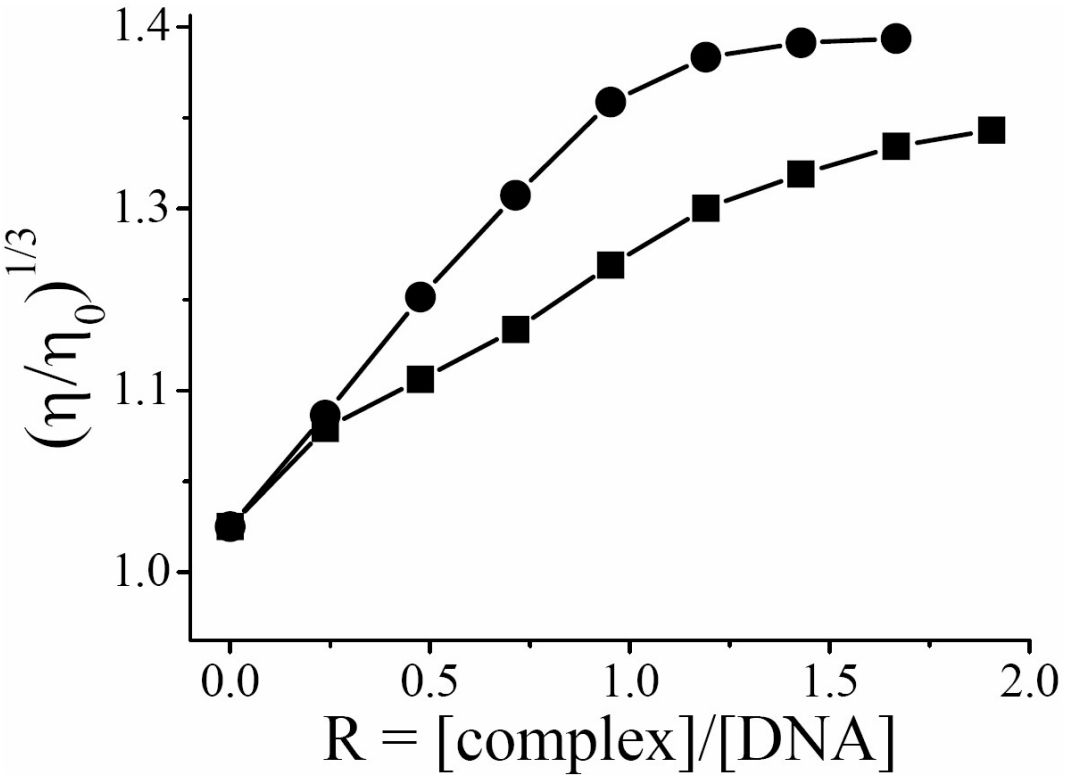

Fig. S8. Effect of increasing the quantity of **1** (■) and **2** (●) on the relative viscosities of CT-DNA at 37.0 (± 0.1) °C in 5 mM Tris-HCl buffer (pH, 7.2) ([DNA] = 140 μM, R = [complex]/[DNA]).

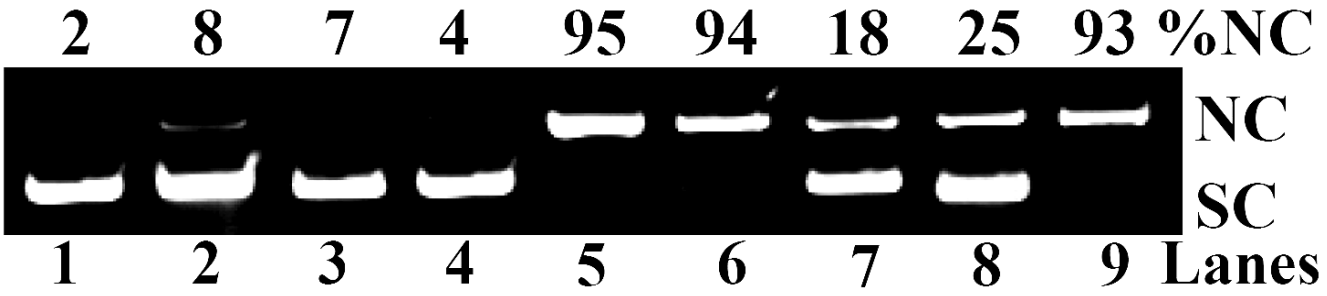

Fig. S9. Gel electrophoresis diagram showing the cleavage of SC pUC19 DNA (0.2 μg, 30 μM) by ligands and metal complexes (2.5 μM) using monochromatic UV-A radiation of 365 nm (6 W) for 1 h exposure time in 50 mM Tris-HCl/NaCl buffer (pH, 7.2) containing 1.5% DMF. Detail conditions are given below in a tabular form.

Lane No.	Reaction conditions	λ / nm	Exposure time(t/min)	%NC
1	DNA	365	60	2
2	dpq	365	60	8
3	dppz	365	60	7
4	DNA + **2** (in dark)	—	60	4
5	DNA + **1**	365	60	95
6	DNA + **2**	365	60	94
7	DNA + distamycin	365	60	18
8	DNA + distamycin + **1**	365	60	25
9	DNA + distamycin + **2**	365	60	93

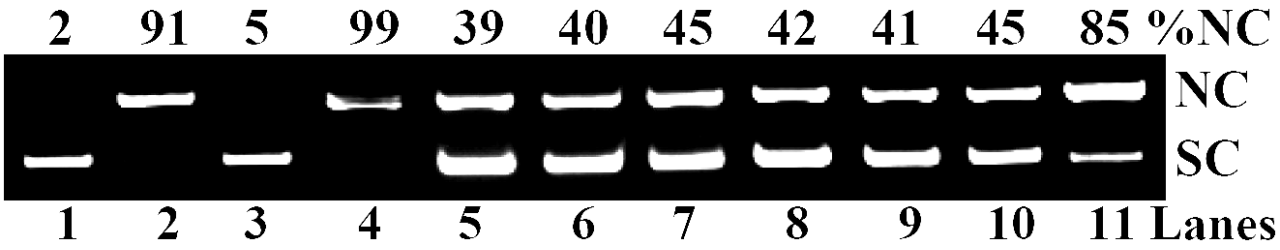

Fig. S10. Gel electrophoresis diagram displaying the photocleavage of SC pUC19 DNA (0.2 μg, 30 μM) at 365 nm by **2** (2.5 μM) in the presence of different additives for 1 h exposure time in 50 mM Tris-HCl/NaCl buffer (pH, 7.2). Detail conditions are given below in a tabular form.

Lane No.	Reaction conditions	λ / nm	Exposure time(t/min)	%NC
1	DNA	365	60	2
2	DNA + **2**	365	60	91
3	DNA + **2** (in argon)	365	60	5
4	DNA + **2** + D_2O	365	60	99
5	DNA + **2** + NaN_3	365	60	39
6	DNA + **2** + TEMP	365	60	40
7	DNA + **2** + DABCO	365	60	45
8	DNA + **2** + DMSO	365	60	42
9	DNA + **2** + KI	365	60	41
10	DNA + **2** + catalase	365	60	45
11	DNA + **2** + SOD	365	60	85

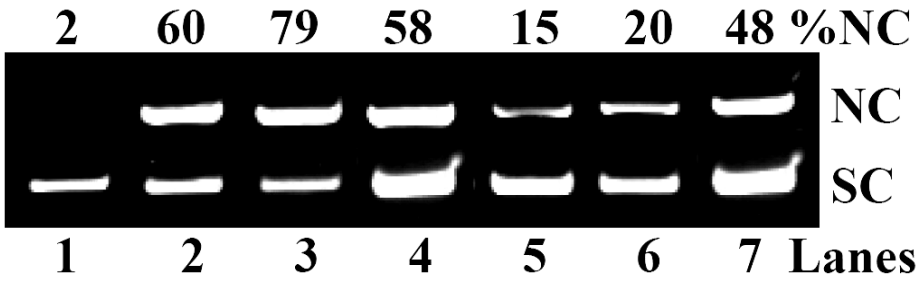

Fig. S11. Gel electrophoresis diagram displaying the photocleavage of SC pUC19 DNA (0.2 μg, 30 μM) by **2** (10 μM) in the presence of different additives for 2 h exposure time in 50 mM Tris-HCl/NaCl buffer (pH, 7.2) on irradiation with red light of λ >750 nm (100 mW). Detail conditions are given below in a tabular form.

Lane No.	Reaction condition	λ / nm	Exposure time (t / h)	%NC
1	DNA	>750	2	2
2	DNA + **2**	>750	2	60
3	DNA + D_2O + **2**	>750	2	79
4	DNA + NaN_3 + **2**	>750	2	58
5	DNA + DMSO + **2**	>750	2	15
6	DNA + Catalase + **2**	>750	2	20
7	DNA + SOD + **2**	>750	2	48

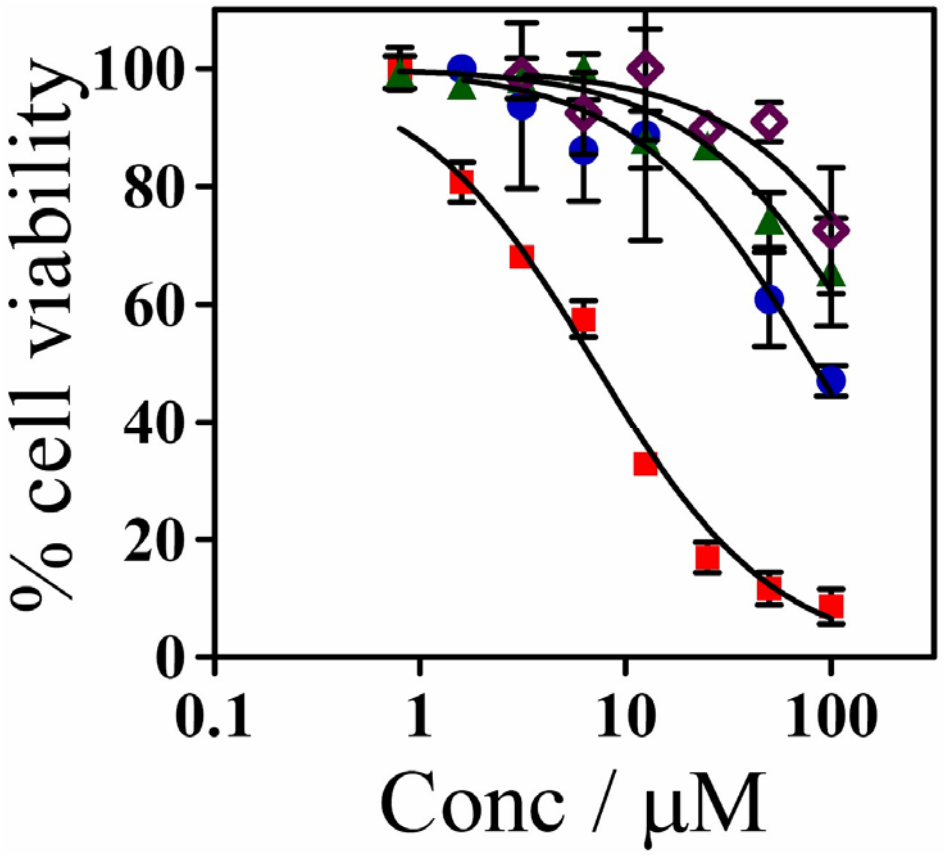

Fig. S12. Photocytotoxicity of $[VOCl(dppz)_2]Cl$ (**2**) (■), dppz ligand (●), dpq ligand (▲) and $VOSO_4$ (◊) in HeLa cells upon incubation for 30 min in dark followed by irradiation with visible light (400 to 700 nm, 20 J cm^{-2}) as determined by MTT assay. The IC_{50} values are 12, 95, >100 and >100 μM, respectively.

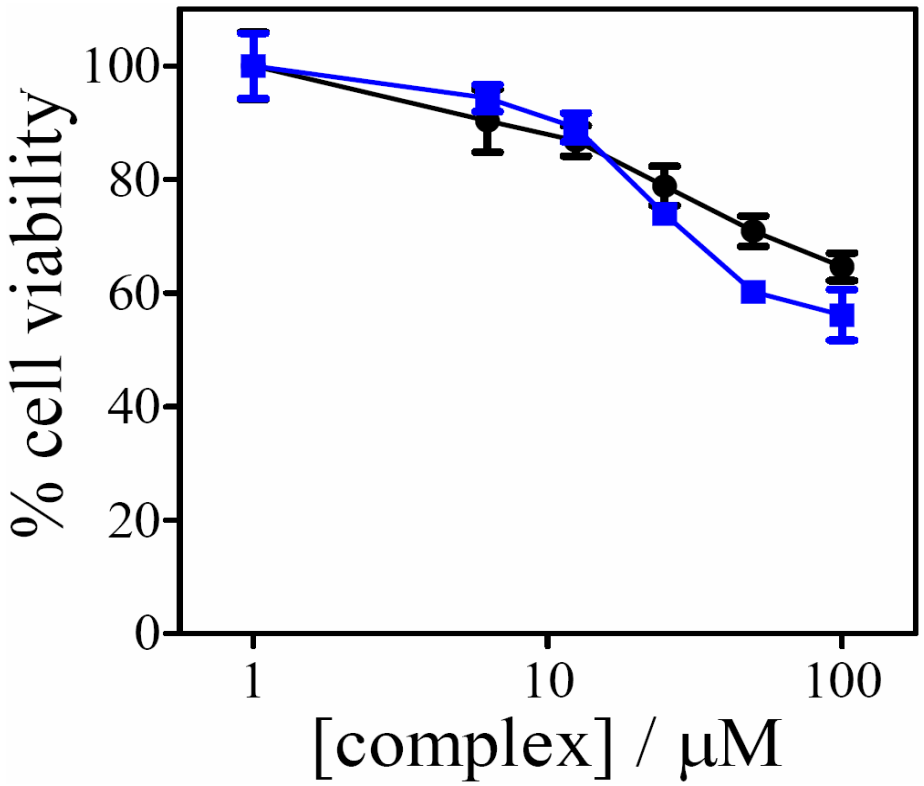

Fig. S13. Photocytotoxicity of the $[VOCl(dpq)_2]Cl$ (**1)** in HeLa cells upon incubation for 30 min in dark followed by irradiation with UV-A light (365 nm, 0.549 J cm^{-2}) as determined by MTT assay. The dark-treated cells are shown by circle (●) and the UV-A light-exposed cells are shown by squares (■). The IC_{50} values in dark and UV-A light are greater than 100 μM.

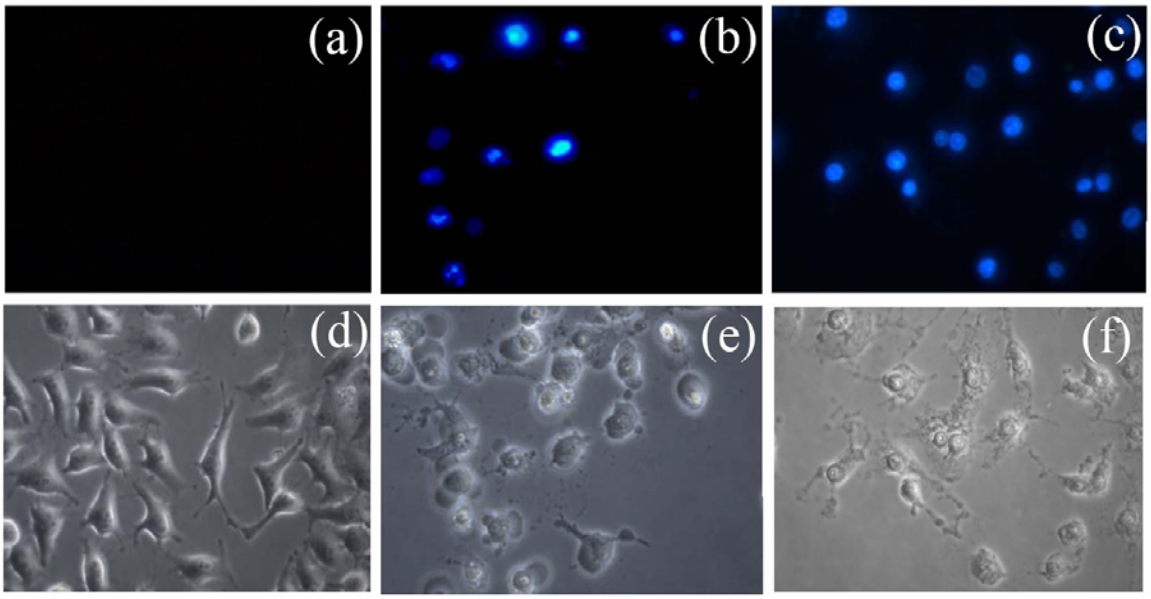

Fig. S14. DAPI staining of nuclei of HeLa cells (2 h post photoexposure) treated with **2** and UV-A light of 365 nm (a) untreated control cells, (b) cells treated with 1 μM of **2**, (c) cells treated with 10 μM of **2**. Panels (a)-(c) are from a fluorescence microscope with 360/40 nm excitation filter and 460/50 nm emission filter. Panels (d)-(f) are the respective bright-field images.

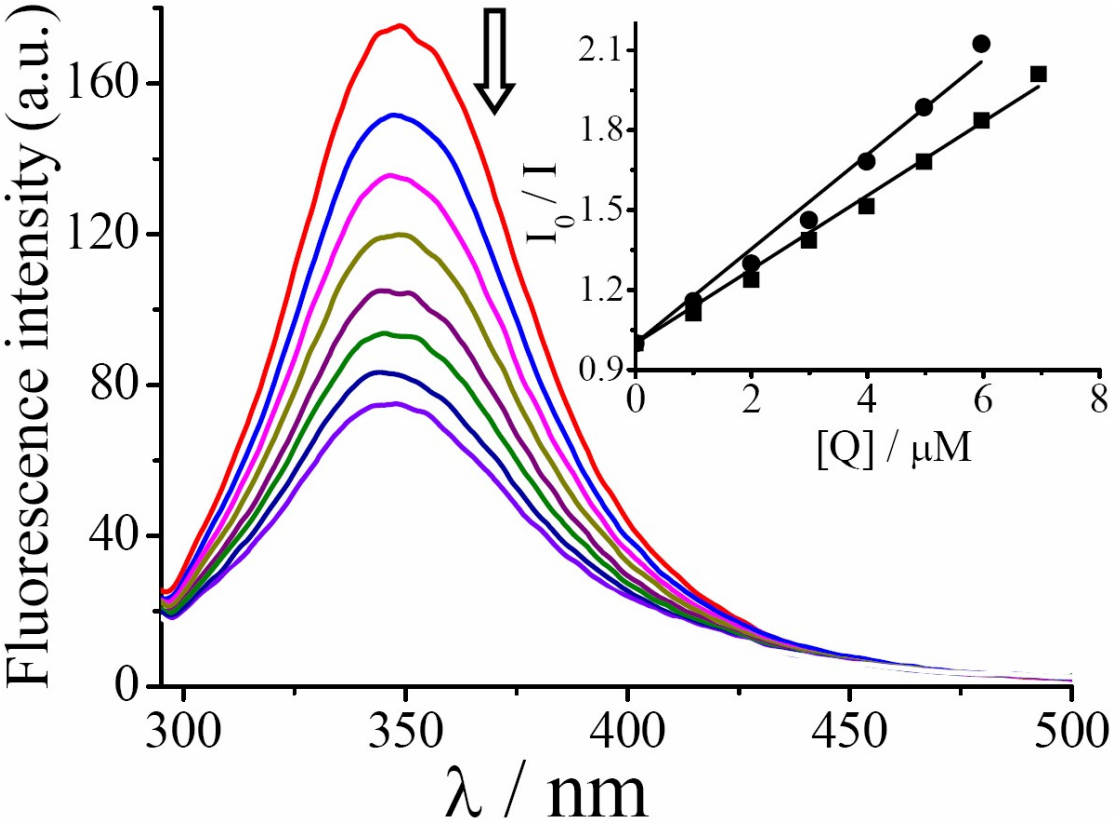

Fig. S15. Emission spectral traces of BSA (2 μM) in the presence of complex **2** with the inset showing the plot of (I_0/I) vs. [complex] for **1** (■) and **2** (●).

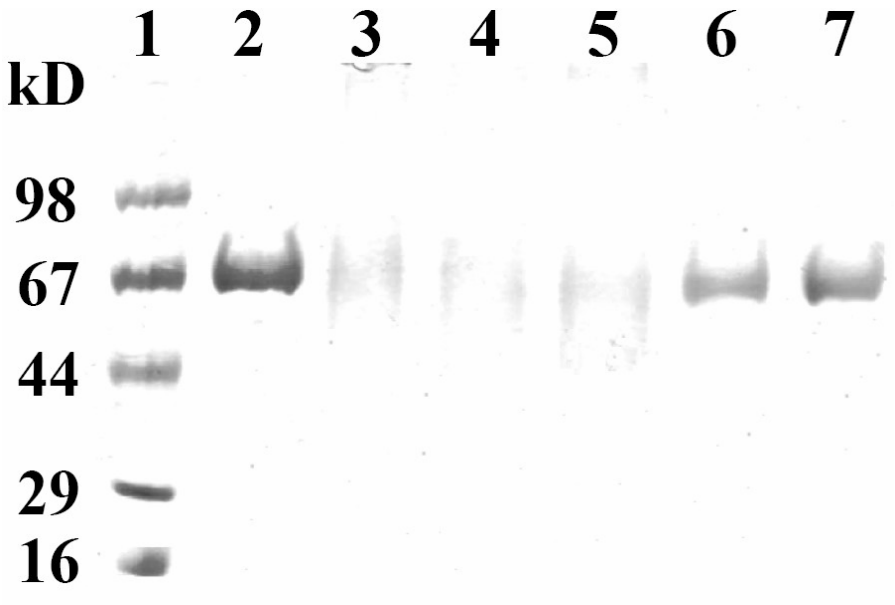

Fig. S16. 12.5% SDS-PAGE of BSA (5 μM) on 2 h photoexposure in UV-A light (365 nm, 6 W) using complex **2** (100 μM) in the presence of different additives in a 0.75% DMF-Tris-HCl buffer (50 mM, pH 7.2) at 25 °C: lane 1, standard molecular weight marker; lane 2, protein control on photoexposure; lane 3, BSA + **2**; lane 4, BSA + **2** + NaN_3; lane 5, BSA + **2** + TEMP; lane 6, BSA + **2** + DMSO; lane 7, BSA + **2** + KI. The singlet oxygen quenchers like NaN_3 and TEMP did not inhibit the cleavage reaction. The hydroxyl radical scavengers like DMSO and KI showed significant inhibition of the photocleavage of BSA indicating the involvement of hydroxyl radicals as the reactive species.